Supporting Information

A Post-modified Donor-Acceptor Covalent Organic Framework for Enhanced Photocatalytic H_2 Production and High Proton Transport

Saiqi Yang [a, ‡], Wei Liu [a, ‡], Yining Zhang [b], Xiaohui Jia [a], Jingyan Sun [a], Chenxi Zhang [a, *], Mingguang Liu [c, *]

‡ These authors contributed equally to this work.

[a] College of Chemical Engineering and Materials Science, Tianjin University of Science and Technology, Tianjin 300457, China

[b] College of Sciences, Tianjin University of Science and Technology, Tianjin 300457, China

[c] Naval Logistics Academy, Tianjin 300450, China

* Corresponding author.

E-mails: 22810017@mail.tust.edu.cn; zcx@tust.edu.cn; 2935267lmg@163.com

Table of Contents

Section 1. Material, Characterizations and Methods

Section 2. Synthetic Procedures

Section 3. Supplementary Figures

Section 4. Supplementary Tables

Section 5. References

Section 1. Material, Characterizations and Methods

Chemicals and reagents

All solvents and reagents obtained from commercial sources were used without further purification. 1,3,6,8-tetrabromopyrene (98 %), N,N-Dimethylformamide (DMF), tetrahydrofuran (THF) were purchased from J&K. 4-formylphenylboronic acid (98 %), 4,7-dibromo-2,1,3-benzothiazolyldiazole (99.8 %) and 4-cyanomethylphenylboronic acid pinacol ester (99 %) were procured from Shanghai Bide Pharmaceutical Technology Co. Ltd. Tetrakis (triphenylphosphine) palladium ($Pd(PPh_3)_4$), o-dichlorobenzene (o-DCB), tetrabutylammonium hydroxide (TBAH), ethanol (EtOH) and hydrogenhexachloroplatinum (IV) hexahydrate ($H_2PtCl_6 \cdot 6H_2O$, 8 *wt*% in water) were acquired from Energy Chemical.

Characterizations

Powder X-ray diffraction (PXRD) patterns were collected for the as-prepared COF samples using the Shimadzu Labx XRD-6100 diffractometer within a 2θ range of 1.5° to 50° with a step size of 0.02°. Ultraviolet-visible diffuse reflectance (UV-vis DR) spectra were recorded on the Shimadzu UV-2700 spectrophotometer, employing $BaSO_4$ as the substrate, over a wavelength range of 200 to 800 nm. Fourier-transform infrared (FT-IR) spectra were collected using the Bruker Tensor 27 spectrometer with a wavenumber range of 400 to 4000 cm^{-1}, using KBr as the substrate. Solid-state ^{13}C cross-polarization magic-angle-spinning nuclear magnetic resonance (^{13}C CP-MAS NMR) spectra were collected by an Agilent-NMR-vnmrs600. N_2 adsorption-desorption isotherms at 77 K were acquired using the Micromeritics ASAP 2020 system subsequent to degassing the COF samples at 110 °C for 12 hours (h). Scanning electron microscopy (SEM) images were obtained using the JEOL-6700F field emission scanning electron microscope equipped with Local energy-dispersive X-ray (EDX). High-resolution transmission electron microscope (HRTEM) images were obtained using the HITACHI HT7800. Thermogravimetric analysis (TGA) was conducted using the SDT-Q600 instrument, ramping the temperature from room temperature (25 °C) to 700 °C at a heating rate of 10 °C/min under a N_2 atmosphere. X-ray photoelectron spectroscopy (XPS) and valence band X-ray photoelectron spectroscopy (VBXPS) measurements were performed on the THERMO SCIENTIFIC ESCALAB 250Xi spectrometer, with the powder material affixed to conductive adhesive under high vacuum. AC impedance and cyclic voltammetry (CV) analyses were recorded using the CHI 760E (Shanghai Chenhua) electrochemical workstation. CV measurements were executed employing a three-electrode system, with Ag/AgCl, Pt and carbon paper coated with COF samples (1 mg cm^{-2} loading) serving as

reference electrode, counter electrode, and working electrode, respectively. The voltage range for testing was from -0.583 to 1.417 V.

Acidity Measurement

Direct titration method was used to determine the acidization degree of PyBT-COF-COOH and the acidity was calculated utilizing the following equation:

$$Acidity = \frac{CVM}{m}$$

where C represents the concentration of standard NaOH solution, V represents the volume of standard NaOH solution consumed during titration (mL), M represents the relative molecular weight of NaOH (40 g/mol) and m represents the weight of PyBT-COF-COOH sample (mg).

Photoelectronic measurements

Mott-Schottky (M-S) measurements and photocurrent analysis of the COFs were also conducted using the CHI 760E electrochemical workstation employing a three-electrode system. A working electrode consisting of indium tin oxide glass coated with COF samples (1 mg cm^{-2} loading) was utilized, with the electrode system immersed in a 0.5 M Na_2SO_4 solution. M-S measurements were performed at frequencies of 1000, 1500 and 2000 Hz. For photocurrent analysis, the working electrode was subjected to irradiation by the 300 W Xenon lamp with a 420 nm cut-off filter. The light-dependent variation in photocurrent intensity was observed through multiple cycles of alternating light and dark tests, each lasting for 20 seconds.

Computational details

The calculations of the energy levels and optimization of fragments of the COFs structure were using density functional theory (DFT) by Gaussian 09 package. The molecular orbitals were obtained at the B3LYP/6-311G (d, p) level. The electron excitation analysis was carried out by Multiwfn.

Photocatalytic Performance Test

Following the dispersion of 20 mg of COF photocatalyst in 100 mL of 0.1M ascorbic acid aqueous solution within a quartz reactor (PerfectLight, Beijing), $H_2PtCl_6 \cdot 6H_2O$ (16 μL) was added. Subsequently, the reactor underwent sonication for 10 minutes, followed by evacuation and purging with N_2 (three times). Prior to the illumination of the mixture under a 300 W Xenon lamp equipped with a 420 nm cut-off filter for 5 h, $H_2PtCl_6 \cdot 6H_2O$ was allowed to deposit in the dark for 1 h to facilitate the *in situ* formation of Pt as a cocatalyst. Throughout the photoreaction, the temperature was maintained to 25 °C via circulating cooling water. Gas samples were periodically withdrawn from the reactor and analyzed

using Shimadzu gas chromatography (GC-2018) with TCD as the detector. Subsequent to the photoreaction, the COF samples were retrieved, washed with water, and dried under vacuum at 80°C overnight in preparation for subsequent long-term cycling photocatalytic assessments following the same protocol.

The apparent quantum efficiency (AQE) of H_2 production for PyBT-COF-COOH was measured following standard photocatalytic test procedure. The mixture underwent irradiation using a 300 W Xenon lamp fitted with various bandpass filters (420 nm, 450 nm, 500 nm and 550 nm) for 5 h. The irradiation area encompassed 28.26 cm^2 (corresponding to the reactor radiation area radius of 3 cm), with a light intensity of 10 mW cm^{-2}. The AQE was computed using the equation provided below:

$$AQE\,(\%) = \frac{2 \times n_e \times N_A \times h \times c}{I \times S \times t \times \lambda} \times 100 \quad (1)$$

where n_e is the amount of generated electrons for H_2, N_A is Avogadro constant (6.022×10^{23} mol^{-1}), h is the Planck constant (6.626×10^{-34} J s), c is the speed of light (3×10^8 m s^{-1}), S is the irradiation area (cm^2), I is the optical density of irradiation light (W cm^{-2}), t is the irradiation time (s), and λ is the monochromatic light wavelength (m).

Proton Conductivity Test

The proton conductivity of PyBT-COF-COOH was evaluated using AC impedance technique under controlled conditions of humidity and temperature. A sheet sample of PyBT-COF-COOH, prepared via tablet pressing and molding under a pressure of 10 MPa, with a diameter of 6 mm and a thickness ranging of 0.5 to 1.0 mm, was secured between the electrodes of a double-electrode cell connected to the electrochemical workstation. Subsequently, the cell was enclosed with a sealed bottle container containing saturated saline solution, alloing for the investigation of the humidity-dependent proton conductivity of PyBT-COF-COOH under varying levels of humidity controlled by the saturated saline solution. The temperature-dependent proton conductivity was examined using Electrochemical impedance spectroscopy (EIS) within a frequency range of 1 Hz to 1 MHz, employing an AC potential of 100 mV, while maintaining the humidity at 98 % RH. The light-dependent proton conductivity was examined under the irradiation of a 300W Xenon lamp equipped with a 420 nm cut-off filter within 5 min. The proton conductivity was determined utilizing the following equation:

$$\sigma = \frac{d}{AR} \quad (2)$$

where σ is the proton conductivity in S cm^{-1}, d is the thickness of the sheet sample of PyBT-COF-COOH, R is the resistance of the COF sample, and A is the cross-sectional area of the tested sample.

The activation energy (E_a) of PyBT-COF-COOH for proton conduction was computed using the equation below:

$$Ln\sigma_T = LnA - \frac{E_a}{K_B T} \quad (3)$$

where σ is the proton conductivity in S cm^{-1}, A is the pre-exponential factor, K_B represents Boltzmann constant, and T is the test temperature (K).

Section 2. Synthetic Procedures

Synthesis of PyTB-4CHO [1]

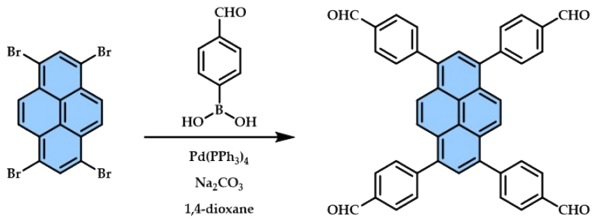

4, 4', 4'', 4'''-(pyrene-1, 3, 6, 8-tetrayl)tetraphenylamine (PyTB-4CHO).

A mixture of 1, 3, 6, 8-tetrabromopyrene (0.54 g, 1.1 mmol), $Pd(PPh_3)_4$ (0.06 g, 0.05 mmol), 4-formylphenyl boronic acid (0.98 g, 6.53 mmol) and K_2CO_3 (2.30 g, 16.64 mmol) was added to 1,4-dioxane (50 mL) under nitrogen atmosphere. The mixture was then kept at 85 ℃ for 48 h. Pour the solution into cold H_2O and neutralized with HCl (2 mL) to dissolve the remaining K_2CO_3. The filtered precipitate was washed with MeOH and then dried to obtain a yellow powder (yield 80 %).

Synthesis of BTDP-2CN [1]

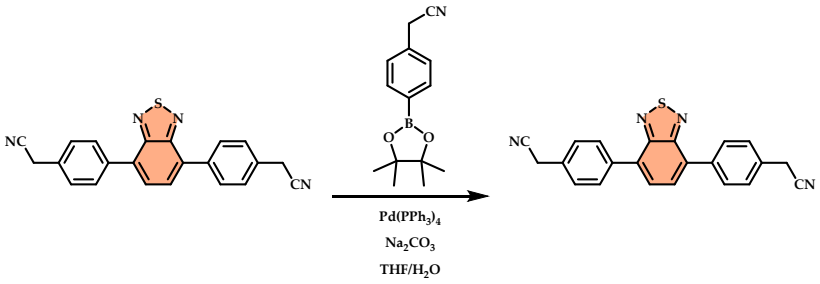

4, 7-bis(4-cyanomethylphenyl)benzothiadiazole (BTDP-2CN).

A mixture of 4,7-Dibromo-2,1,3-benzothiazolyldiazole (0.4 g, 0.82 mmol), 4-cyanomethylphenylboronic acid pinacol ester (1 g, 2.46 mmol), sodium carbonate (1.1 g, 6.2mmol), tetrakis (triphenylphosphine) palladium (0.12 g, 0.06 mmol) was added to the mixed solvent of 40 mL tetrahydrofuran (THF) and 10 mL water. Then the mixture was heated to 80 ℃ reflux for 24 h under N_2 atmosphere. After cooling down to room temperature, pour into the water and filter, the crude product was purified by column chromatography (with dichloromethane as eluent) to give compound as a yellow-green powder (yield 82 %).

^{1}H NMR of monomers

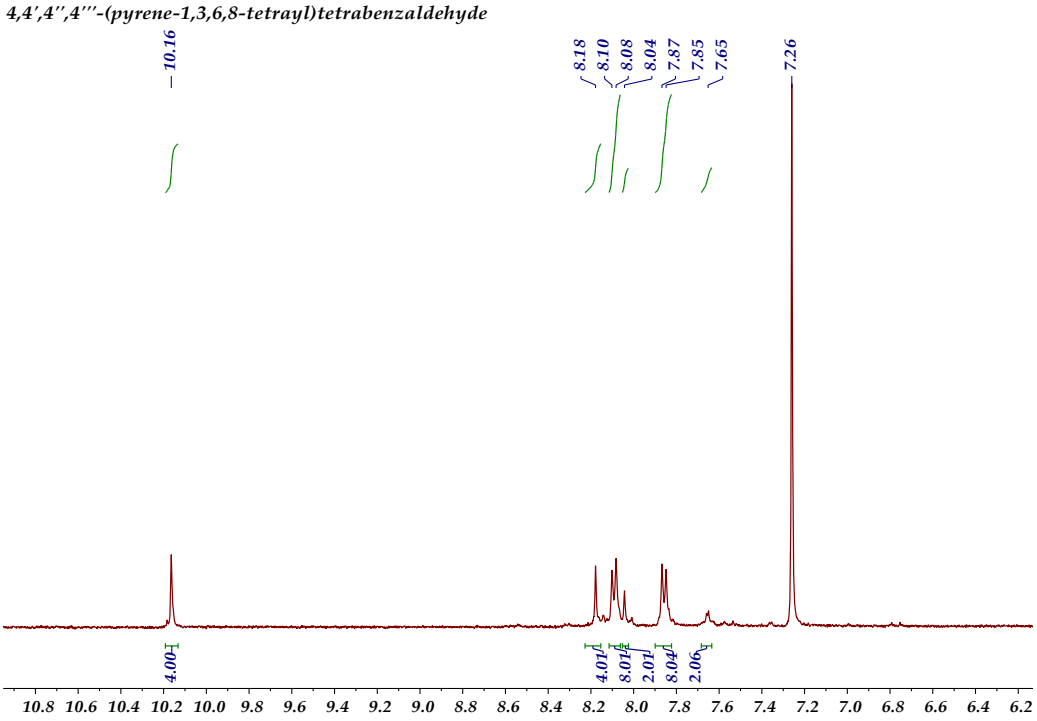

^{1}H NMR spectra of PyTB-4CHO in $CDCl_3$.

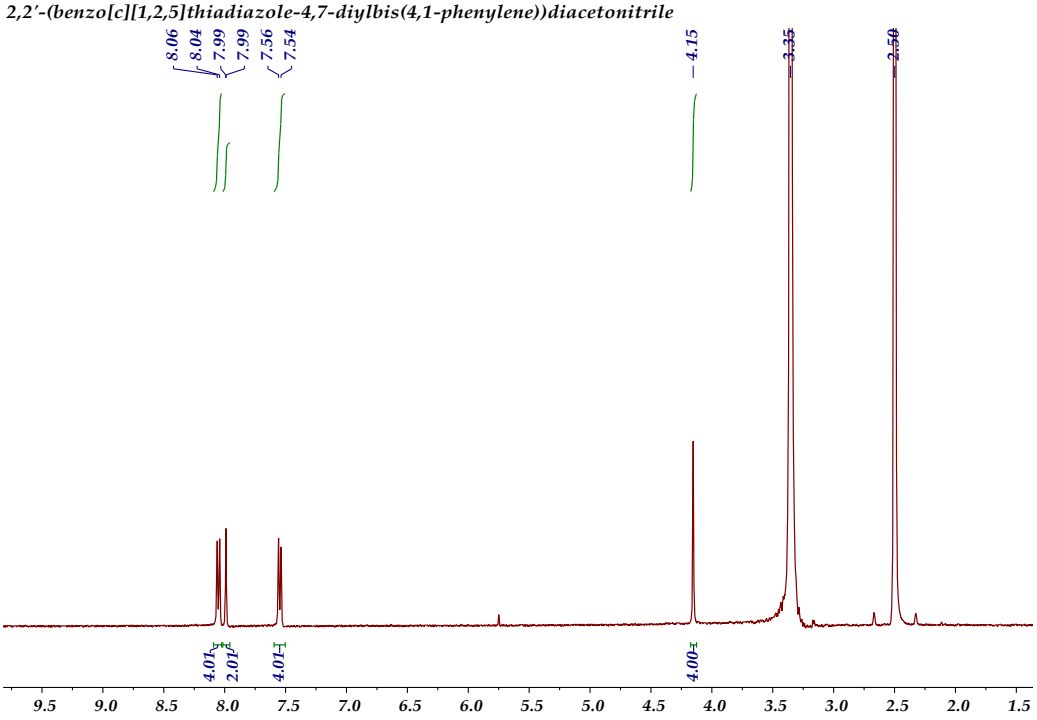

^{1}H NMR spectra of BTDP-2CN in DMSO-d6.

Synthesis of COFs

PyBT-COF was prepared via a Knoevenagel condensation reaction involving the electron-rich pyrene (Py) moiety and the electron-deficient benzothiadiazole (BT) moiety. Specifically, a mixture comprising Py-4CHO (20.0 mg, 0.032 mmol) and BTDP-2CN (24.0 mg, 0.065 mmol) was introduced into o-DCB (2 mL) within a Schlenk tube. Subsequently, the tube underwent sonication for 15 minutes, followed by the addition of 0.2 mL of 1 M TBAH in methanol as the reaction catalyst, and 0.1 mL of water for dilution. After subjecting the mixture to three cycles of freeze-thaw operations, the tube was vacuum-sealed and heated to 120 ^{o}C for 72 h. The resulting precipitate was washed with N, N-dimethylformamide (DMF), 1 M HCl aqueous solution, water, and tetrahydrofuran (THF), and subsequently, it was subjected to Soxhlet extraction with THF/Acetone as a rinsing solvent for 24 h to remove oligomeric impurities. Finally, PyBT-COF powder was collected as an orange solid after drying at 80 ^{o}C under vacuum for 12 h. The post-modification of PyBT-COF to **PyBT-COF-COOH** was achieved as follows: PyBT-COF solid (100.0 mg) was introduced into a 25 mL Schlenk tube containing a 20 % NaOH solution (H_2O/EtOH, v/v = 1/1, 10 mL). The mixture was then heated to 80 ^{o}C for three days under a N_2 atomspheer. The solid was filtered and refluxed in water for 2 h followed by refluxing in 1 M HCl aqueous solution for additional 2 h. The resulting sample was collected, washed with water and THF, and then subjected to Soxhlet extraction with THF/Acetone as a rinsing solvent for 24 h to remove captured guest molecules. The final product was collected and dried under vacuum at 80 ^{o}C, yielding PyBT-COF-COOH as a light orange powder.

Section 3. Supplementary Figures

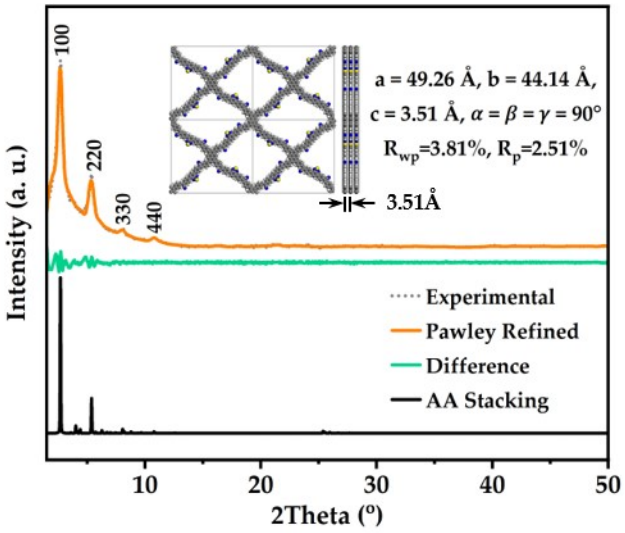

Fig. S1 PXRD pattern of PyBT-COF.

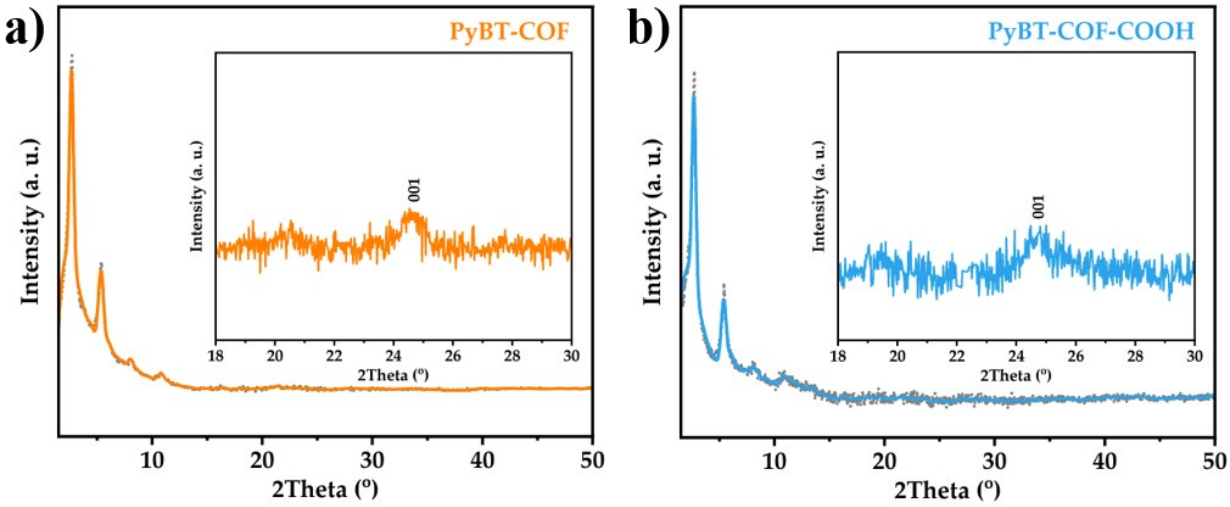

Fig. S2 Experimental PXRD patterns of a) PyBT-COF and b) PyBT-COF-COOH. Insert: enlarged diffraction peaks corresponding to the (001) lattice place of the two COFs.

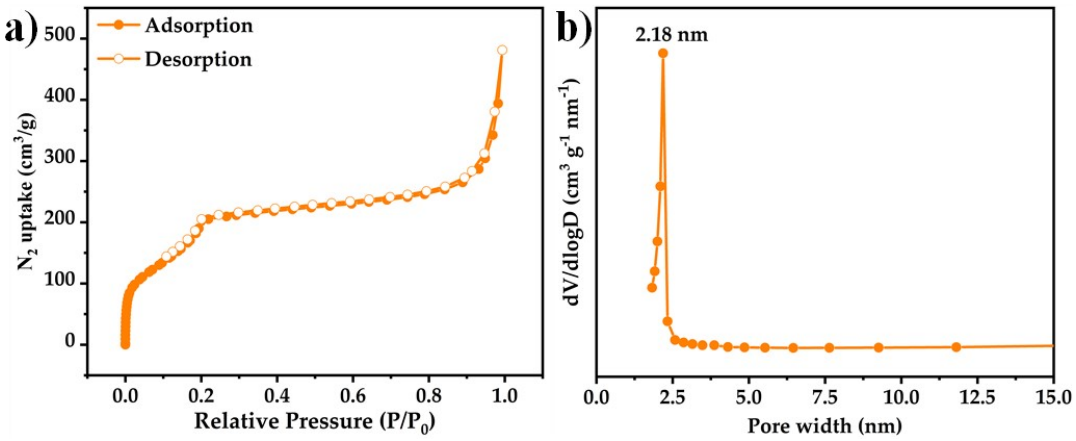

Fig. S3 a) N_2 adsorption and desorption isotherms of PyBT-COF. b) The pore-size distribution of PyBT-COF.

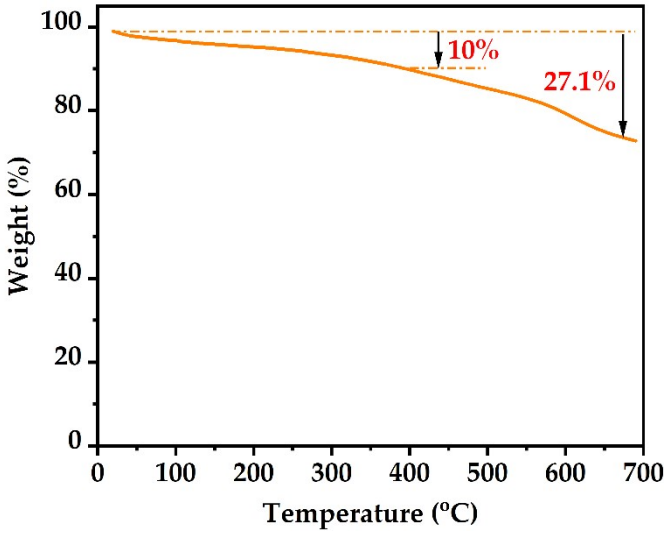

Fig. S4 TGA curve of PyBT-COF.

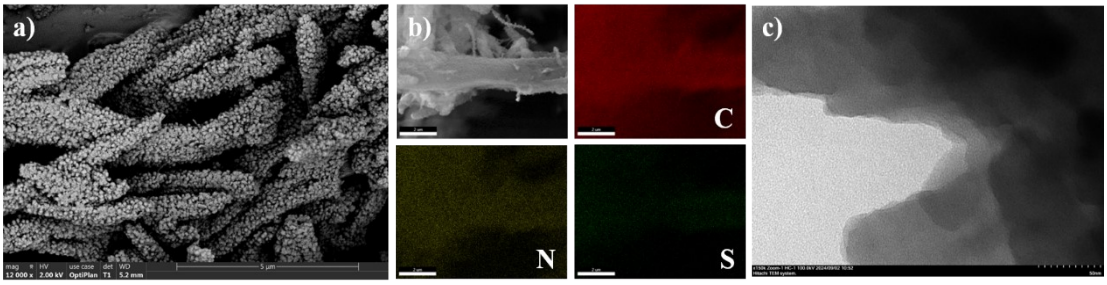

Figure S5. a) SEM image and b) the elemental mapping spectra of PyBT-COF. c) HRTEM image of PyBT-COF.

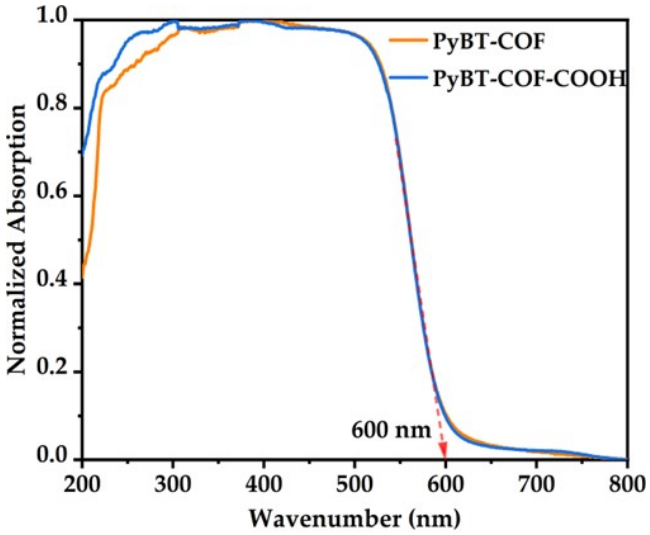

Fig. S6 Normalized absorption spectra of PyBT-COF and PyBT-COF-COOH.

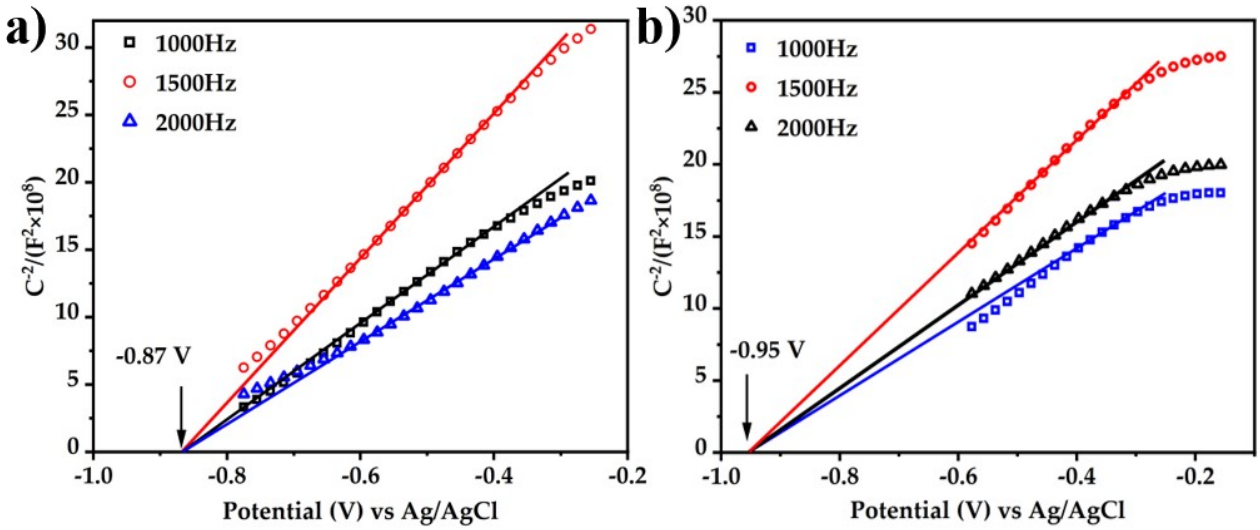

Fig. S7 Mott-Schottky plots for a) PyBT-COF and b) PyBT-COF-COOH.

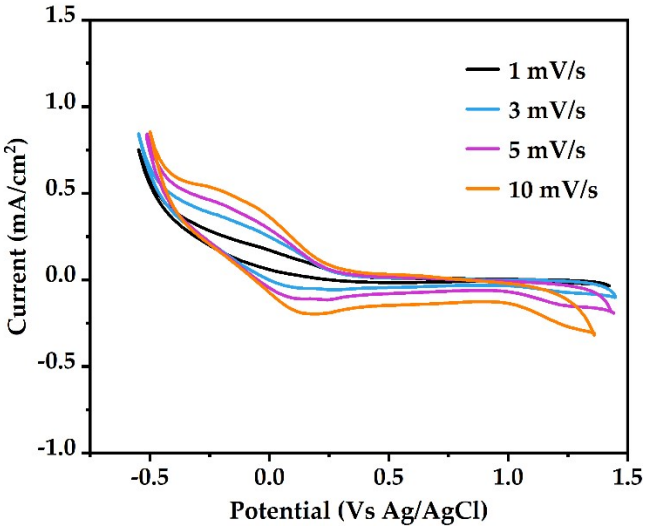

Fig. S8 CV test of PyBT-COF with different scanning rate and 1.0 M Na_2SO_4 aqueous solution as electrolyte.

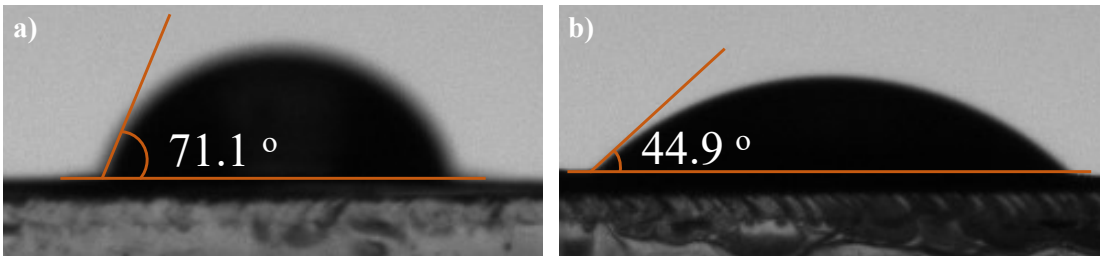

Fig. S9 Water contact angle measurements of a) PyBT-COF and b) PyBT-COF-COOH at room temperature in air.

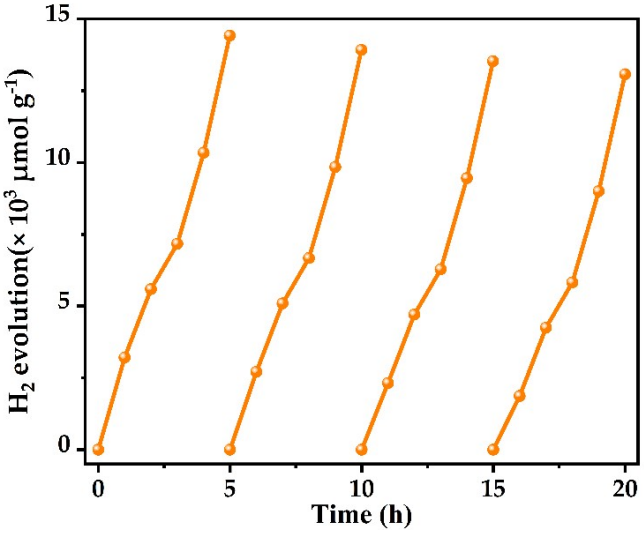

Fig. S10 Cyclic photocatalytic hydrogen production of PyBT-COF for a total duration of 20 h.

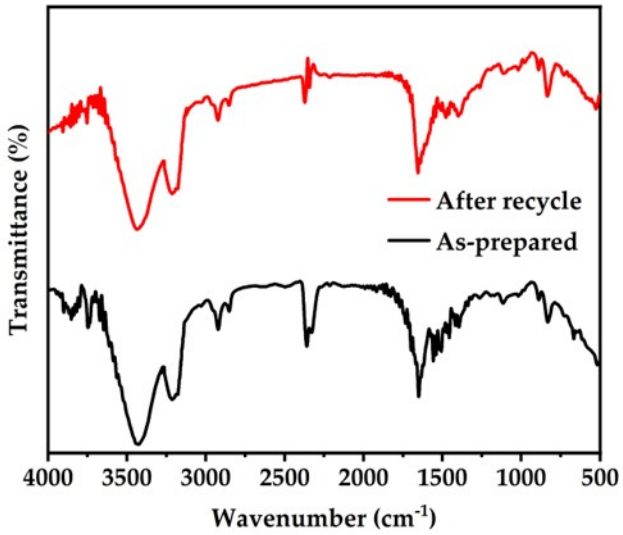

Fig. S11 FT-IR spectra of as-prepared PyBT-COF-COOH and after recycle.

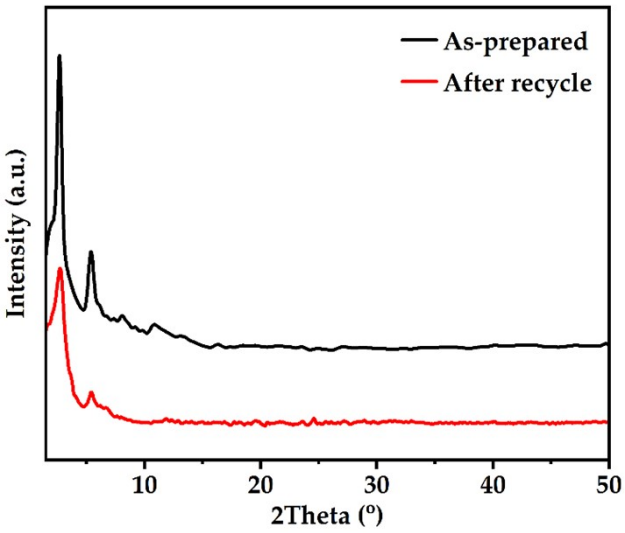

Fig. S12 PXRD pattern of as-prepared PyBT-COF-COOH and after recycle.

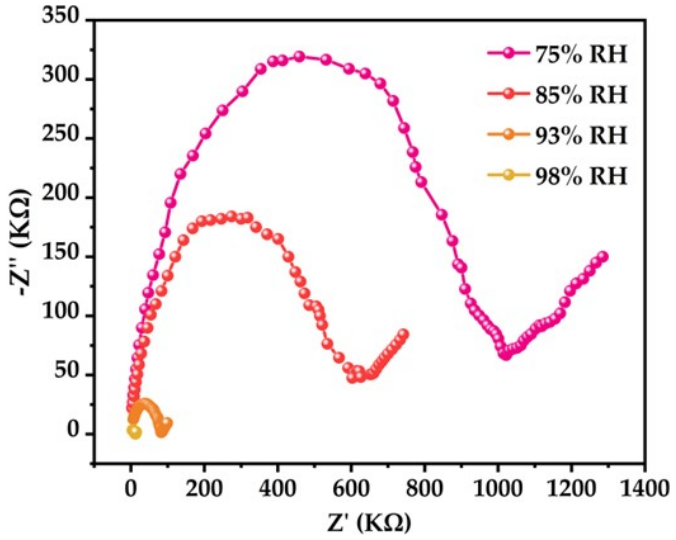

Fig. S13 Nyquist plots of PyBT-COF-COOH under different RH at 293 K.

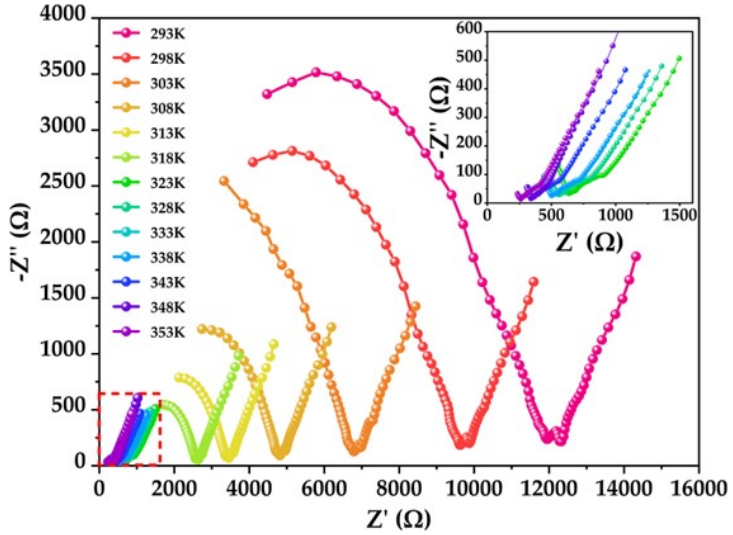

Fig. S14 Nyquist plots of PyBT-COF-COOH under 98 % RH at different temperatures.

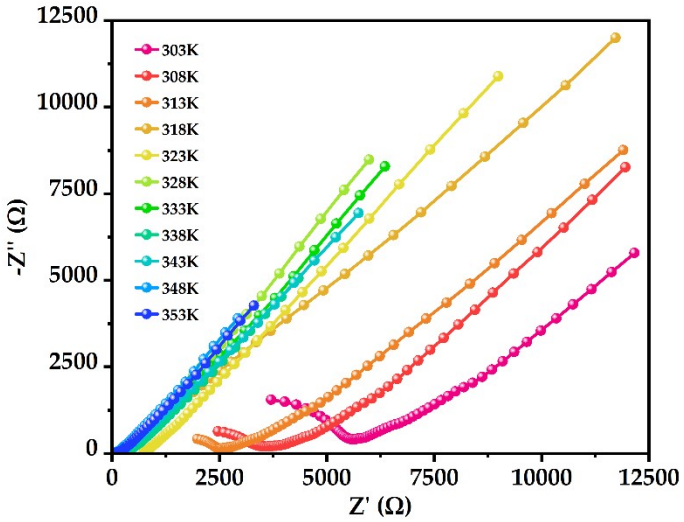

Fig. S15 Nyquist plots of PyBT-COF-COOH under 98 % RH and light irradiation at different temperatures.

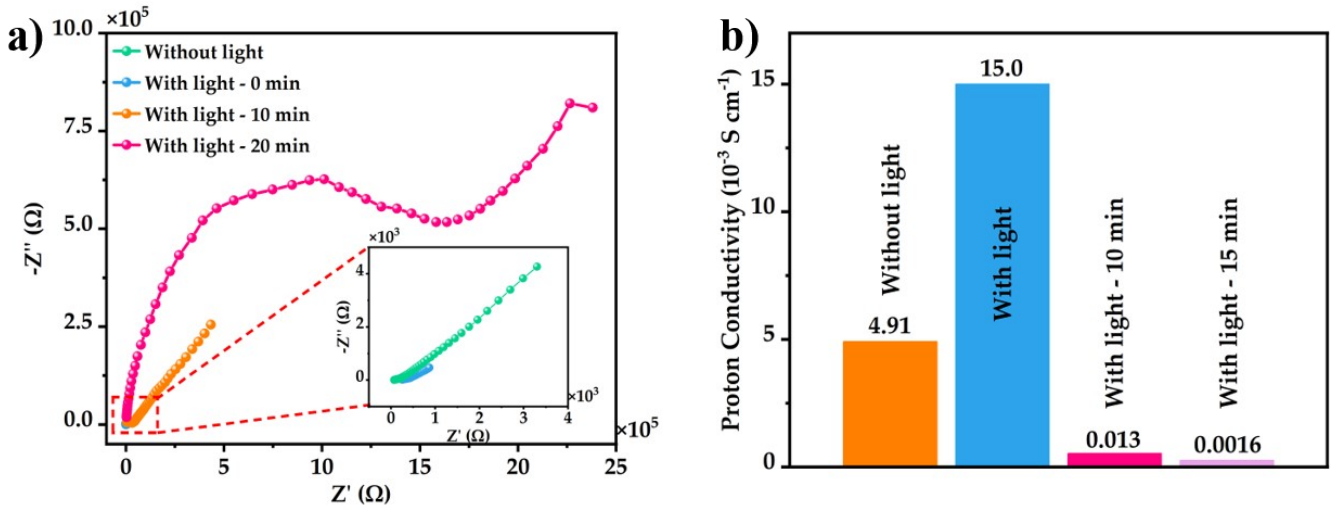

Fig. S16 a) Nyquist plots of PyBT-COF-COOH under 98 % RH and light irradiation for different time at 353 K. b) Proton conductivity of PyBT-COF-COOH under 98 % RH and light irradiation for different time at 353 K.

Section 4. Supplementary Tables

Table S1 The acidity measurement of PyBT-COF-COOH based on direct titration method.

order	*C* (mol/L)	*V* (mL)	*m* (g)	acidity (mg_{NaOH}/g)	average acidity (mg_{NaOH}/g)
1	0.0103	2.413	0.050	19.883	19.904
2	0.0103	2.405	0.050	19.817	
3	0.0103	2.428	0.050	20.006	
4	0.0103	2.410	0.050	19.858	
5	0.0103	2.422	0.050	19.957	

Table S2 Fractional atomic coordinates for the simulated unit cells of PyBT-COF with AA stacking mode.

PyBT-COF with AA Stacking							
Space group: P2/m a = 49.26 Å, b = 44.14 Å, c = 3.51 Å				α = β = γ = 90 °			
Atom	x/a	y/b	z/c	Atom	x/a	y/b	z/c
C1	0.45119	0.48334	0.5	N73	0.23977	0.6778	0.5
C2	0.47563	0.46729	0.5	N74	0.27859	0.18046	0.5
C3	0.50029	0.48384	0.5	S75	0.31291	0.18188	0.5
C4	0.47447	0.53176	0.5	N76	0.31205	0.22018	0.5
C5	0.4506	0.51474	0.5	N77	0.06751	0.7874	0.5
C6	0.52388	0.56485	0.5	N78	0.16896	0.06604	0.5
C7	0.49864	0.5793	0.5	C79	0.1042	0.11302	0.5
C8	0.47385	0.56391	0.5	C80	0.08818	0.87026	0.5
C9	0.54857	0.58472	0.5	C81	0.07916	0.12784	0.5
C10	0.44853	0.58295	0.5	C82	0.05503	0.11124	0.5
C11	0.45076	0.61472	0.5	C83	0.05534	0.07937	0.5
C12	0.42774	0.63316	0.5	C84	0.08066	0.06483	0.5
C13	0.40171	0.62042	0.5	C85	0.10476	0.08135	0.5
C14	0.39922	0.58888	0.5	C86	0.09314	0.90143	0.5
C15	0.42231	0.57041	0.5	C87	0.07161	0.92208	0.5
C16	0.57501	0.5729	0.5	C88	0.0445	0.91219	0.5
C17	0.5976	0.5919	0.5	C89	0.03976	0.88076	0.5

C18	0.59436	0.62338	0.5	C90	0.06124	0.86012	0.5
C19	0.56818	0.63549	0.5	C91	0.95004	0.98839	0.5
C20	0.54557	0.61642	0.5	C92	0.97306	0.96991	0.5
C21	0.61739	0.64471	0.5	C93	0.99897	0.98388	0.5
C22	0.37653	0.63879	0.5	C94	0.97718	0.03423	0.5
C23	0.37384	0.66917	0.5	C95	0.95203	0.01972	0.5
C24	0.39723	0.689	0.5	C96	0.02909	0.06215	0.5
C25	0.34629	0.68295	0.5	C97	0.00514	0.07913	0.5
C26	0.64415	0.63872	0.5	C98	0.97919	0.06632	0.5
C27	0.66366	0.66429	0.5	H99	0.43105	0.47061	0.5
C28	0.65447	0.60804	0.5	H100	0.43006	0.52664	0.5
N29	0.41586	0.70498	0.5	H101	0.49749	0.6051	0.5
N30	0.66284	0.58354	0.5	H102	0.47164	0.62585	0.5
C31	0.6917	0.65883	0.5	H103	0.43003	0.65886	0.5
C32	0.71009	0.68287	0.5	H104	0.37824	0.57798	0.5
C33	0.70095	0.71299	0.5	H105	0.42005	0.54471	0.5
C34	0.67291	0.71839	0.5	H106	0.57829	0.54734	0.5
C35	0.65449	0.6944	0.5	H107	0.61891	0.5818	0.5
C36	0.34322	0.71456	0.5	H108	0.56517	0.66109	0.5
C37	0.31746	0.72776	0.5	H109	0.52425	0.62647	0.5
C38	0.29396	0.70978	0.5	H110	0.6135	0.67017	0.5
C39	0.29704	0.67816	0.5	H111	0.35588	0.62714	0.5
C40	0.32282	0.66489	0.5	H112	0.69965	0.63457	0.5
C41	0.26663	0.72441	0.5	H113	0.73285	0.67817	0.5
C42	0.72089	0.7383	0.5	H114	0.66491	0.74262	0.5
C43	0.26471	0.75622	0.5	H115	0.63174	0.69915	0.5
C44	0.23943	0.77086	0.5	H116	0.36191	0.72981	0.5
C45	0.21504	0.75429	0.5	H117	0.3153	0.75347	0.5
C46	0.21727	0.72242	0.5	H118	0.27837	0.6629	0.5
C47	0.24202	0.70809	0.5	H119	0.32493	0.63917	0.5
C48	0.2512	0.26836	0.5	H120	0.28421	0.77012	0.5
C49	0.23174	0.24525	0.5	H121	0.2384	0.79666	0.5
C50	0.23943	0.21457	0.5	H122	0.24407	0.29293	0.5
C51	0.26748	0.20821	0.5	H123	0.20921	0.25115	0.5

C52	0.28654	0.23085	0.5	H124	0.20779	0.81595	0.5
C53	0.18856	0.77076	0.5	H125	0.16324	0.84415	0.5
C54	0.21803	0.1908	0.5	H126	0.11932	0.75746	0.5
C55	0.18799	0.80259	0.5	H127	0.16389	0.72936	0.5
C56	0.16334	0.81832	0.5	H128	0.81533	0.77584	0.5
C57	0.13854	0.80261	0.5	H129	0.85208	0.81557	0.5
C58	0.13912	0.77083	0.5	H130	0.79	0.88709	0.5
C59	0.16375	0.75518	0.5	H131	0.75322	0.84724	0.5
C60	0.80945	0.80082	0.5	H132	0.13174	0.86269	0.5
C61	0.82984	0.82273	0.5	H133	0.12371	0.15695	0.5
C62	0.82329	0.85367	0.5	H134	0.07833	0.15365	0.5
C63	0.79584	0.8621	0.5	H135	0.03467	0.1235	0.5
C64	0.77547	0.84013	0.5	H136	0.08178	0.03903	0.5
C65	0.11215	0.819	0.5	H137	0.12511	0.06905	0.5
C66	0.08731	0.80151	0.5	H138	0.1149	0.91023	0.5
C67	0.11184	0.84952	0.5	H139	0.07589	0.94746	0.5
C68	0.15509	0.12297	0.5	H140	0.01808	0.87173	0.5
C69	0.12897	0.1318	0.5	H141	0.05693	0.83475	0.5
C70	0.83726	0.90868	0.5	H142	0.92894	0.97778	0.5
N71	0.19639	0.70289	0.5	H143	0.93254	0.03365	0.5
S72	0.20697	0.66644	0.5	H144	0.00612	0.10494	0.5

Table S3 Fractional atomic coordinates for the simulated unit cells of PyBT-COF-COOH with AA stacking mode.

PyBT-COF-COOH with AA Stacking							
Space group: P2/m a = 47.43Å, b = 45.22Å, c = 3.50Å				α = β = γ = 90 °			
Atom	x/a	y/b	z/c	Atom	x/a	y/b	z/c
H1	0.78079	0.95207	0.5	S77	0.32551	0.19436	0.5
H2	0.94411	0.24803	0.5	N78	0.31775	0.23087	0.5
H3	0.57974	0.25439	0.5	C79	0.07775	0.86253	0.5
H4	0.71174	0.57212	0.5	C80	0.08631	0.89222	0.5
C5	0.44804	0.48919	0.5	C81	0.06645	0.91527	0.5
C6	0.47187	0.47096	0.5	C82	0.03733	0.90935	0.5

C7	0.49887	0.48429	0.5	C83	0.02902	0.87953	0.5
C8	0.47642	0.53365	0.5	C84	0.04885	0.85674	0.5
C9	0.4502	0.51977	0.5	O85	0.16956	0.05265	0.5
C10	0.53052	0.56025	0.5	O86	0.21172	0.07118	0.5
C11	0.5058	0.57707	0.5	O87	0.33625	0.42846	0.5
C12	0.47871	0.56494	0.5	O88	0.29634	0.4051	0.5
C13	0.55781	0.5768	0.5	O89	0.40284	0.72997	0.5
C14	0.45443	0.58647	0.5	O90	0.43285	0.69409	0.5
C15	0.4602	0.61694	0.5	O91	0.07736	0.76173	0.5
C16	0.43858	0.63782	0.5	O92	0.05026	0.80009	0.5
C17	0.41029	0.62944	0.5	C93	0.94731	0.99464	0.5
C18	0.40421	0.59906	0.5	C94	0.96929	0.97401	0.5
C19	0.42592	0.57787	0.5	C95	0.99738	0.98447	0.5
C20	0.58404	0.56248	0.5	C96	0.97974	0.03594	0.5
C21	0.6091	0.57854	0.5	C97	0.95235	0.02482	0.5
C22	0.60856	0.60934	0.5	C98	0.03608	0.05681	0.5
C23	0.5826	0.62385	0.5	C99	0.01306	0.07616	0.5
C24	0.55754	0.60785	0.5	C100	0.98495	0.06685	0.5
C25	0.63355	0.62847	0.5	C101	0.11874	0.09681	0.5
C26	0.3861	0.65063	0.5	C102	0.09443	0.11422	0.5
C27	0.3832	0.68064	0.5	C103	0.06781	0.10118	0.5
C28	0.4074	0.70231	0.5	C104	0.06487	0.07029	0.5
C29	0.35331	0.69231	0.5	C105	0.08949	0.0531	0.5
C30	0.66181	0.62502	0.5	C106	0.11605	0.06616	0.5
C31	0.67792	0.65351	0.5	H107	0.42606	0.47897	0.5
C32	0.6769	0.59587	0.5	H108	0.43009	0.53358	0.5
C33	0.70748	0.65427	0.5	H109	0.50705	0.60224	0.5
C34	0.72214	0.681	0.5	H110	0.48296	0.62504	0.5
C35	0.70765	0.70802	0.5	H111	0.44385	0.66242	0.5
C36	0.67742	0.70742	0.5	H112	0.38137	0.59121	0.5
C37	0.66325	0.68059	0.5	H113	0.42054	0.5533	0.5
C38	0.3477	0.72282	0.5	H114	0.5851	0.5373	0.5
C39	0.32024	0.73388	0.5	H115	0.63021	0.56649	0.5
C40	0.29699	0.71479	0.5	H116	0.58179	0.64905	0.5

C41	0.30223	0.68419	0.5	H117	0.53645	0.61994	0.5
C42	0.3299	0.67312	0.5	H118	0.63098	0.65353	0.5
C43	0.26779	0.72741	0.5	H119	0.36353	0.64196	0.5
C44	0.72335	0.73633	0.5	H120	0.72	0.63275	0.5
C45	0.26403	0.75833	0.5	H121	0.74617	0.68105	0.5
C46	0.23701	0.7711	0.5	H122	0.66501	0.729	0.5
C47	0.21256	0.75347	0.5	H123	0.63922	0.68014	0.5
C48	0.21666	0.7225	0.5	H124	0.36587	0.73933	0.5
C49	0.24313	0.71004	0.5	H125	0.31648	0.75877	0.5
C50	0.24706	0.26426	0.5	H126	0.28387	0.66792	0.5
C51	0.23146	0.23808	0.5	H127	0.33371	0.64823	0.5
C52	0.24485	0.21033	0.5	H128	0.28353	0.77306	0.5
C53	0.27452	0.21005	0.5	H129	0.2346	0.79618	0.5
C54	0.28984	0.23572	0.5	H130	0.23544	0.28633	0.5
C55	0.18408	0.76782	0.5	H131	0.20744	0.23896	0.5
C56	0.22727	0.18323	0.5	H132	0.20083	0.81342	0.5
C57	0.18125	0.7988	0.5	H133	0.15265	0.83732	0.5
C58	0.15452	0.81219	0.5	H134	0.11353	0.74928	0.5
C59	0.12969	0.79505	0.5	H135	0.16125	0.72571	0.5
C60	0.13291	0.76418	0.5	H136	0.81224	0.79119	0.5
C61	0.15942	0.75084	0.5	H137	0.84308	0.83648	0.5
C62	0.8021	0.81405	0.5	H138	0.76786	0.89305	0.5
C63	0.81916	0.83897	0.5	H139	0.73696	0.84768	0.5
C64	0.80754	0.8676	0.5	H140	0.12076	0.85239	0.5
C65	0.77807	0.87023	0.5	H141	0.13869	0.13698	0.5
C66	0.76088	0.84517	0.5	H142	0.10971	0.89796	0.5
C67	0.10078	0.8092	0.5	H143	0.07384	0.93926	0.5
C68	0.07498	0.78969	0.5	H144	0.00566	0.87357	0.5
C69	0.10019	0.83934	0.5	H145	0.04157	0.83271	0.5
C70	0.17337	0.10603	0.5	H146	0.92448	0.98678	0.5
C71	0.14564	0.11285	0.5	H147	0.93363	0.04064	0.5
C72	0.81477	0.92471	0.5	H148	0.01671	0.10108	0.5
N73	0.19609	0.70214	0.5	H149	0.09625	0.13936	0.5
S74	0.20901	0.66727	0.5	H150	0.04812	0.11563	0.5

N75	0.24241	0.68039	0.5	H151	0.08796	0.02794	0.5
N76	0.2908	0.18579	0.5	H152	0.13577	0.05175	0.5

Table S4. The photocatalysis performance of HER comparison of PyBT-COF-COOH with other COF-based materials.

COF	Sacrificial agent	Light absorption range (nm)	H_2 evolution ($\mu mol\ g^{-1}\ h^{-1}$)	Ref.
PyBT-COF-COOH	Ascorbic acid	~ 600	8150	This work
PyBT-COF	Ascorbic acid	~ 600	2884	This work
$En_{TAPT\text{-}TDOE}$	Ascorbic acid	~ 620	2396	[2]
TM-DMA-COF	Ascorbic acid	~ 530	4300	[3]
BTTh-TZ-COF	Ascorbic acid	~ 546	5220	[4]
TpBD COF@ZIS-10	Ascorbic acid	~ 650	7551	[5]
COF-OH-2	Ascorbic acid	~ 640	2910	[6]
$CN/COF_{4.88}$	TEOA	~ 700	7788	[7]
$COF\text{-}AD_1\text{-}Co\text{-}2$	TEOA	~ 730	7072	[8]

Table S5. The proton conduction comparison of PyBT-COF-COOH with other COF-based materials.

COF	σ ($S\ cm^{-1}$)	Condition	E_a (eV)	Ref.
PyBT-COF-COOH (light irradiation)	1.50×10^{-2}	98 % RH, 353 K	0.41	This work
PyBT-COF-COOH	4.91×10^{-3}	98 % RH, 353 K	0.49	This work
PyPz-COF	1.74×10^{-3}	98 % RH, 353 K	0.34	[9]
H_3PO_4@ PyPz-COF-2 M	1.28×10^{-2}	98 % RH, 353 K	0.20	
2D-polymer POPM	2.80×10^{-3}	98 % RH, 353 K	0.33	[10]
His@TpTta	3.45×10^{-3}	100 % RH, 373 K	0.34	[11]
NH_4Br@COF-Im^+-SO_3^-	3.69×10^{-3}	100 % RH, 363 K	0.45	[12]
C6-[dema]HSO_4-1.0	2.84×10^{-3}	413 K	0.38	[13]
EB-COF:PW_{12}	3.32×10^{-6}	456 K	0.13	[14]
Aza-COF-1_H	1.23×10^{-3}	97 % RH, 323 K	0.29	[15]
Aza-COF-2_H	4.81×10^{-3}	97 % RH, 323 K	0.42	
$[Cu(p\text{-}IPhHIDC)]_n$	1.51×10^{-3}	98 % RH, 373 K	0.25	[16]

Section 5. References

[1] J. Cheng; Y. Wu; W. Zhang; J. Zhang; L. Wang; M. Zhou; F. Fan; X. Wu; H. Xu. Fully Conjugated 2D sp^2 Carbon-Linked Covalent Organic Frameworks for Photocatalytic Overall Water Splitting. *Advanced Materials* **2024**, 36, 2305313.

[2] X. Guan; Y. Qian; X. Zhang; H.-L. Jiang. Enaminone-Linked Covalent Organic Frameworks for Boosting Photocatalytic Hydrogen Production. *Angew. Chem. Int. Ed.* **2023**, 62, e202306135.

[3] Z. Xie; X. Yang; P. Zhang; X. Ke; X. Yuan; L. Zhai; W. Wang; N. Qin; C.-X. Cui; L. Qu; X. Chen. Vinylene-linked covalent organic frameworks with manipulated electronic structures for efficient solar-driven photocatalytic hydrogen production. *Chin. J. Catal.* **2023**, 47, 171-180.

[4] H. Liu; X. Zheng; J. Xu; X. Jia; M. Chao; D. Wang; Y. Zhao. Structural Regulation of Thiophene-Based Two-Dimensional Covalent Organic Frameworks toward Highly Efficient Photocatalytic Hydrogen Generation. *ACS Appl. Mater. Interfaces* **2023**, 15, 16794-16800.

[5] S. Bao; Q. Tan; S. Wang; J. Guo; K. Lv; S. A. C. Carabineiro; L. Wen. TpBD COF@$ZnIn_2S_4$ nanosheets: A novel S-scheme heterojunction with enhanced photoreactivity for hydrogen production. *Appl. Catal., B* **2023**, 330, 122624.

[6] Y. Chen; X. Luo; J. Zhang; L. Hu; T. Xu; W. Li; L. Chen; M. Shen; S.-B. Ren; D.-M. Han; G.-H. Ning; D. Li. Bandgap engineering of covalent organic frameworks for boosting photocatalytic hydrogen evolution from water. *J. Mater. Chem. A* **2022**, 10, 24620-24627.

[7] J. Ding; Y. Lou; G. Dong; Y. Zhang. Covalent organic framework films grown on spongy g-C_3N_4 for efficient photocatalytic hydrogen production. *J. Photochem. Photobiol., A* **2023**, 439, 114590.

[8] D. Aand; S. Sk; K. Kumar; U. Pal; A. K. Singh. Boosting photocatalytic hydrogen generation by the combination of tunable cobaloxime and covalent organic framework. *Int. J. Hydrogen Energy* **2022**, 47, 7180-7188.

[9] F. D. Wang; L. J. Yang; X. X. Wang; Y. Rong; L. B. Yang; C. X. Zhang; F. Y. Yan; Q. L. Wang. Pyrazine-Functionalized Donor–Acceptor Covalent Organic Frameworks for Enhanced Photocatalytic H_2 Evolution with High Proton Transport. *Small* **2023**, 2207421.

[10] H. Zhong; G. Wu; Z. Fu; H. Lv; G. Xu; R. Wang. Flexible Porous Organic Polymer Membranes for Protonic Field-Effect Transistors. *Adv. Mater.* **2020**, 32, 2000730.

[11] T. Zhang; Y. Xia; Y.-D. Xie; H.-J. Du; Z.-Q. Shi; H.-L. Hu; H. Zhang; Z.-C. Guo; G. Li. Superprotonic conductivity of ketoenamine covalent-organic frameworks grafted by imidazole-based units. *J. Colloid Interface Sci.* **2024**, 665, 554-563.

[12]S. Bian; K. Zhang; Y. Wang; Z. Liu; G. Wang; X. Jiang; Y. Pan; B. Xu; G. Huang; G. Zhang. Charge Separation by Imidazole and Sulfonic Acid-Functionalized Covalent Organic Frameworks for Enhanced Proton Conductivity. *ACS Appl. Energy Mater.* **2022**, 5, 1298-1304.

[13]X. Wu; Z. Liu; H. Guo; Y.-l. Hong; B. Xu; K. Zhang; Y. Nishiyama; W. Jiang; S. Horike; S. Kitagawa; G. Zhang. Host–Guest Assembly of H-Bonding Networks in Covalent Organic Frameworks for Ultrafast and Anhydrous Proton Transfer. *ACS Applied Materials & Interfaces* **2021**, 13, 37172-37178.

[14]H. Ma; B. Liu; B. Li; L. Zhang; Y.-G. Li; H.-Q. Tan; H.-Y. Zang; G. Zhu. Cationic Covalent Organic Frameworks: A Simple Platform of Anionic Exchange for Porosity Tuning and Proton Conduction. *J. Am. Chem. Soc.* **2016**, 138, 5897-5903.

[15]Z. Meng; A. Aykanat; K. A. Mirica. Proton Conduction in 2D Aza-Fused Covalent Organic Frameworks. *Chem. Mater.* **2019**, 31, 819-825.

[16]Z. Sun; S. Yu; L. Zhao; J. Wang; Z. Li; G. Li. A Highly Stable Two-Dimensional Copper(II) Organic Framework for Proton Conduction and Ammonia Impedance Sensing. *Chemistry – A European Journal* **2018**, 24, 10829-10839.